Available online at www.sciencedirect.com
SCIENCE DIRECT®
Journal of Photochemistry and Photobiology A: Chemistry 163 (2004) 223–230
Journal of Photochemistry and Photobiology A:Chemistry
www.elsevier.com/locate/jphotochem

A novel hyperbranched polyisophthalate used as polymeric binders in holographic diffraction gratings☆

Huiguang Kou [a], Wenfang Shi [a,*], Yonghua Lu [b], Hai Ming [b]

[a] *Department of Polymer Science and Engineering, University of Science and Technology of China, Hefei, Anhui 230026, PR China*
[b] *Department of Physics, University of Science and Technology of China, Hefei, Anhui 230026, PR China*

Received 12 June 2003; received in revised form 21 November 2003; accepted 28 November 2003

Abstract

A novel photopolymerizable hyperbranched polyisophthalate (HPIP-A) was synthesized from 1,3,5-benzenetricarboxylic acid as a "core" molecule, 5-hydroxyisophthalic acid as an AB_2 monomer, and 2-hydroxyethyl acrylate as an endcapping reagent. This material containing the unsaturation concentration of 5.29 $mmol_{C=C}\ g^{-1}$ measured by ^1H NMR has a wide molecular weight distribution of 2.05 and a degree of branching of 0.45. The refractive index at the wavelength of 650 nm was measured to be 1.562 using an autoretarder ellipsepsometer. The diffraction efficiency (DE) of holographic diffraction grating in the cured film was found to be strongly dependent on writing beam intensity, film thickness, monomer structure and content added in the resin. For a 25 μm thickness HPIP-A film added 30 wt.% methyl acrylate, a high diffraction efficiency of 92.3% was obtained at the writing beam intensity of 0.4 mW cm^{-2}.

Keywords: Photopolymerization–diffusion model; Photopolymerizable recording dry film; Photopolymerizable hyperbranched polyisophthalate; Holographic diffraction grating

1. Introduction

Holography has been widely used in many areas, such as non-destructive testing, information storage, integrated optics, and so on [1–4]. As a kind of holographic recording materials, photopolymerizable recording dry films have recently attracted extensive attention because of their favorable advantages, such as self-developing capability, dry processing, response for visible light, high diffraction efficiency (DE) and spatial frequency, compared with traditional recording materials, such as silver halide, photoresists, thermoplastics, and so on [5–13]. Moreover, the resulting diffraction gratings can be monitored in real time [14–17]. Usually, a photopolymerizable recording dry film is composed of a polymeric binder with higher refractive index (RI) and a monomer with lower RI, as well a photoinitiator. The theory concerning the formation of a holographic diffraction grating in a film is based on the photopolymerization–diffusion model, which was formulated mathematically by Adhami et al. [18]. The recording process in a film is accomplished by the copolymerization of a monomer and a polymeric binder under a nonuniform exposure pattern, which can be obtained with the holographic two-beam interference technique using coherent laser sources [19]. The mechanism of RI modulation is outlined briefly in Fig. 1. The difference in RIs of the bright regions and dark ones, resulting from the different monomer concentration, explains the existence of a modulation index (Δn), i.e. holographic diffraction grating.

In order to obtain a holographic diffraction grating with high performance, the properties of a polymeric binder, such as viscosity, reactivity and compatibility with monomers, are very crucial [20,21]. The so-termed hyperbranched polymers, which grow by repeated reactions of multifunctional monomers, e.g. AB_2 with a "one-pot" procedure, different from classical polymers by their compact molecular shape, high degree of branching, and high density of terminal functionality. These characteristics provide low viscosity, good compatibility with monomers, and high reactivity [22]. Fréchet and coworkers described the orthogonal synthesis of dendritic polyester with regular molecular structure based upon 5-(hydroxymethyl) isophthalic acid (or 3,5-dihydroxy-benzoic acid) via a convergent procedure [23]. Turner and coworkers synthesized the hyperbranched aromatic polyester based upon 5-hydroxyisophthalic acid

☆ Granted by National Natural Science Foundation of China (Nos.: 50233030 and 20074034).
* Corresponding author. Fax: +86-551-3606630.
E-mail address: wfshi@ustc.edu.cn (W. Shi).

1010-6030/$ – see front matter © 2004 Elsevier B.V. All rights reserved.
doi:10.1016/j.jphotochem.2003.11.004

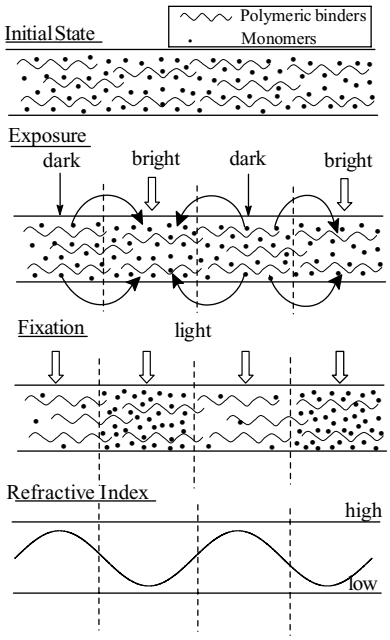

Fig. 1. Mechanism of the refractive index modulation.

proceeding in a "step-wise" growth manner without the addition of "initiator core" for viscosity-regulating applications [24]. However, little work has been performed to prepare photopolymerizable recording dry films with hyperbranched polymers as polymeric binders.

In present work, the photopolymerizable hyperbranched polyisophthalate (HPIP-A) was prepared, and characterized by Fourier transition infrared (FTIR), nuclear magnetic resonance (NMR), and gel permeation chromatography (GPC). The degree of branching (DB) was determined by NMR method using model compounds. The photopolymerizable recording dry films were designed using the synthesized oligomer as a polymeric binder. As the most important parameter of the obtained gratings, DE was investigated by writing beam intensity, film thickness, and monomer structure and content in the film, in real time.

2. Experimental

2.1. Materials

1,3,5-Benzenetricarboxylic acid (BTCA), 5-hydroxyisophthalic acid (HIPA) and dimethylaminopyridine (DMAP) were supplied from Aldrich, Germany. Resorcinol, *m*-phthalic acid, 2-hydroxyethyl acrylate (HEA), methyl acrylate (MA) and methyl methacrylate (MMA) were supplied from Shanghai Shanhu Chemical Co., China. 1,6-Hexanediol diacrylate (HDDA) and trimethylolpropane triacrylate (TMPTA) were supplied from UCB. Co., Belgium. Titanocene derivative (Irgacure 784) as a photoinitiator was supplied from Ciba-Geigy, Switzerland. $SOCl_2$ and other chemicals were supplied from Shanghai First Reagent Co., China, and used after purification with standard methods.

2.2. Measurements

The FTIR spectra were recorded on a MAGNA 750 apparatus (Nicolet Instrument Co., USA). The ^{1}H NMR and ^{13}C NMR spectra were recorded on a DMX-500 apparatus (Brucker Co., Switzerland) using $CDCl_3$ as a solvent. The molecular weight distribution was measured on a Water 150C GPC apparatus equipped with 10^3, 10^4, 10^5 Å columns using polystyrene as a standard, and THF (1.0 ml min^{-1}) as a solvent. The compatibility of the obtained product with monomer MA was determined on a dynamic mechanical thermal analyzer (Rheome Tric SCI Apparatus Ltd., USA). The RI was measured with a V-VASE autoretarder ellipsepsometer (J.A. Woollam Co., USA) in the wavelength range of 240–1100 nm at 25 °C.

2.3. Synthesis

2.3.1. HPIP-A

$SOCl_2$ (3.8 ml) solution in toluene (10 ml) was slowly dropped into the reaction vessel containing BTCA (0.32 g, 1.5 mmol) and HIPA (2.46 g, 13.5 mmol), as well a catalytic amount of DMF, and stirred at 130 °C under nitrogen atmosphere until the wide band for –OH and –COOH groups at the range of 2550–3450 cm^{-1} in the IR spectrum disappeared. Finally, residual $SOCl_2$ and solvent toluene were removed under a vacuum system, yielding a colorless liquid (3.57 g, 96%), named HPIP, which was endcapped with acyl chloride groups.

IR (NaCl): 1735 cm^{-1} (ester carbonyl), 1761 cm^{-1} (acyl chloride carbonyl).

^{1}H NMR (500 MHz, $CDCl_3$): 8.79–8.76 (s, Ar–H, 1.4H), 8.45–8.39 (s, Ar–H, 4.9H), 8.34–8.30 (s, Ar–H, 2.7H), 8.10–7.83 (s, Ar–H, 21H) ppm. The non-integer H values were obtained due to the DB of HPIP.

^{13}C NMR (125 MHz, $CDCl_3$): 169.21, 167.35, 164.98, 162.76, 153.73–151.81, 148.62, 138.45, 135.92, 132.47–130.72, 128.16–125.49, 119.12 ppm.

HEA (2.10 g, 18 mmol) solution in CH_2Cl_2 (10 ml) containing catalytic amounts of DMAP and triethylamine was dropped into the above resultant HPIP, and stirred at 60 °C under nitrogen atmosphere until the band for –OH group around 3300 cm^{-1} and the peak for acyl chloride group at 1761 cm^{-1} in the IR spectrum disappeared. The solution was extracted with HCl (2 M) and $NaHCO_3$ (sat.) solution, and dried over Na_2SO_4 and filtered. Finally, the solvents were removed under a vacuum system, yielding a yellowish liquid (4.1 g, 95%), named HPIP-A, which was terminally capped with acrylic double bonds.

IR (NaCl): 815, 1410, 1615 cm^{-1} (acrylic unsaturation), 1735 cm^{-1} (ester carbonyl).

^{1}H NMR (500 MHz, $CDCl_3$): 9.15–7.84 (s, Ar–H, 30H), 6.40 (d, –C(=O)–CH=CH_2, *cis* to carbony, 11H), 6.12 (t,

–C(=O)–CH=CH_2, 11H), 5.78 (d, –C(=O)–CH=CH_2, *trans* to carbony, 11H), 4.75 (t, –O–CH_2–CH_2–O–C(=O)–Ar, 22H), 4.37 (t, –O–CH_2–CH_2–O–C(=O)–Ar, 22H) ppm.

^{13}C NMR (125 MHz, $CDCl_3$): 172.34, 169.20, 167.35, 162.76, 152.54, 148.78, 138.45, 132.47–130.72, 128.16–125.49, 63.17, 62.70 ppm.

2.3.2. Linear polyphthalate (LPP-A)

In order to investigate the effect of the molecular structure of a polymeric binder on holographic diffraction gratings, the counterpart of HPIP-A, linear polyphthalate (LPP-A) was synthesized as following: $SOCl_2$ (2.5 ml) solution in toluene (10 ml) was dropped into the reaction vessel containing *m*-phthalic acid (1.83 g, 11 mmol) and resorcinol (1.10 g, 10 mmol) as well a catalytic amount of DMF, and stirred at 130 °C under nitrogen atmosphere until the wide band for –OH and –COOH groups at the range of 2550–3450 cm^{-1} in the IR spectrum disappeared. The residual $SOCl_2$ and solvent toluene were removed under a vacuum system. Then, HEA (0.23 g, 2 mmol) solution in CH_2Cl_2 (10 ml) containing catalytic amounts of DMAP and triethylamine was dropped into the above reactant, and stirred at 60 °C under nitrogen atmosphere until the band for –OH group around 3300 cm^{-1} and the peak for acyl chloride group at 1761 cm^{-1} in the IR spectrum disappeared. The solution was extracted with HCl (2 M) and $NaHCO_3$ (sat.) solution, and dried over Na_2SO_4 and filtered. Finally, the solvents were removed under a vacuum system, yielding a viscous yellowish liquid (2.5 g, 90%), named LPP-A, which was terminally capped with acrylic double bonds.

IR (NaCl): 815, 1410, 1615 cm^{-1} (acrylic unsaturation), 1735 cm^{-1} (ester carbonyl).

^{1}H NMR (500 MHz, $CDCl_3$): 8.63 (s, Ar–H, 9H), 8.41 (s, Ar–H, 2H), 8.12 (d, Ar–H, 18H), 7.91 (d, Ar–H, 2H), 7.51–7.39 (d, Ar–H, 21H), 7.14 (d, Ar–H, 18H), 7.05 (s, Ar–H, 9H), 6.40 (d, –C(=O)–CH=CH_2, *cis* to carbony, 2H), 6.12 (t, –C(=O)–CH=CH_2, 2H), 5.76 (d, –C(=O)–CH=CH_2, *trans* to carbony, 2H), 4.70 (t, –O–CH_2–CH_2–O–C(=O)–Ar, 4H), 4.42 (t, –O–CH_2–CH_2–O–C(=O)–Ar, 4H) ppm.

^{13}C NMR (125 MHz, $CDCl_3$): 166.01, 163.05, 162.46, 148.65, 133.15, 132.93, 131.86, 129.80–129.27, 128.55, 117.99, 114.44, 63.17, 62.70 ppm.

2.3.3. Model compounds

The synthesis of three model compounds was described by authors in a previous article and schematically outlined in Fig. 2 [25]. The data of their ^{1}H NMR spectra are given as.

Model compound A: ^{1}H NMR (500 MHz, $CDCl_3$): 8.76 (s, Ar–H, 1H), 8.13 (s, Ar–H, 2H), 7.83 (s, Ar–H, 2H), 7.49 (s, Ar–H, 2H), 7.43 (s, Ar–H, 1H) ppm.

Model compound B: ^{1}H NMR (500 MHz, $CDCl_3$): 8.42 (s, Ar–H, 1H), 8.13 (s, Ar–H, 2H), 8.06 (s, Ar–H, 2H), 7.49 (s, Ar–H, 2H), 7.43 (s, Ar–H, 2H), 7.33 (s, Ar–H, 2H), 7.15 (s, Ar–H, 2H) ppm.

Model compound C: ^{1}H NMR (500 MHz, $CDCl_3$): 8.32 (s, Ar–H, 1H), 8.13 (s, Ar–H, 2H), 8.06 (s, Ar–H, 2H), 7.94 (s, Ar–H, 2H), 7.49 (s, Ar–H, 2H), 7.43 (s, Ar–H, 4H), 7.33 (s, Ar–H, 1H), 7.15 (s, Ar–H, 4H) ppm.

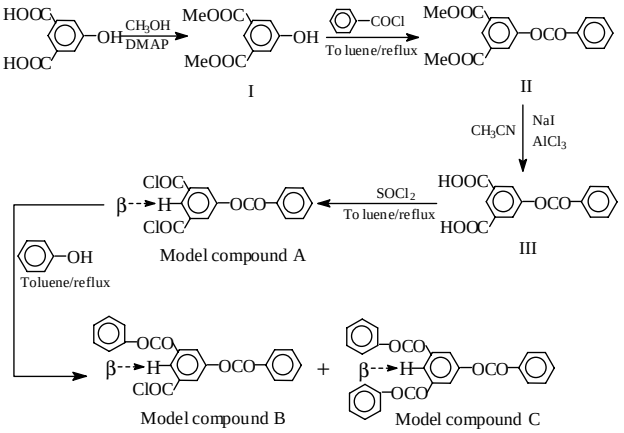

Fig. 2. Schematic description for the synthesis of three model compounds.

2.4. Sample preparation

A given amount of HPIP-A (or LPP-A), monomer (MA, MMA, HEA, HDDA or TMPTA), and 0.5 wt.% (over the total amount of HPIP-A (or LPP-A) and monomer) Irgacure 784 added in CH_2Cl_2 were poured on a quartz glass (20 mm × 20 mm × 1 mm), and layed for 24 h at room temperature, finally, heated at 30 °C under a vacuum system to remove CH_2Cl_2 completely. After that, another quartz glass was placed on the top of the sample to produce a sandwich layer arrangement. The thickness of the sample was controlled by a definite thickness of Teflon spacer between two glasses. The preparation process was performed under a red light in order to prevent the samples from photopolymerization.

2.5. Laser-induced diffraction gratings

The schematic diagram of experimental setup used for monitoring the growth of holographic diffraction gratings is shown in Fig. 3. The above obtained sample exposed to the interference pattern produced by two intersecting Nd:YVO_5

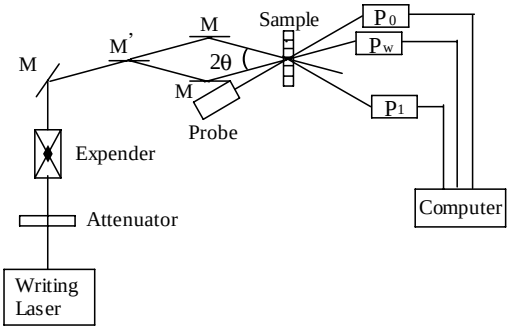

Fig. 3. Schematic diagram of experimental setup used for monitoring the growth of holographic diffraction gratings.

double frequency lasers (532 nm) with the same angle to the sample. The intensities of two beams are equal with a 50:50 beam-splitter M′. For the intersecting angle 2θ of 30°, a grating period of 1.06 μm (grating frequency of 940 mm^{-1}) was obtained. A red low-power (1 mW) semiconductor laser (650 nm) was used to measure the first-order diffraction intensity at Bragg angle (18°, calculated from Bragg condition) in real time, with a field of view of 2°. The intensity of writing beam, the first-order diffracted intensity and the transmitted intensity were recorded with the digital power meters P_w, P_1 and P_0, respectively. The DE is defined as the ratio of the first-order diffraction intensity over the transmitted intensity through the sample before recording.

3. Results and discussion

3.1. Characteristics

3.1.1. Molecular weight distribution and the degree of branching

The reaction scheme for the synthesis of HPIP-A, which ideally contains 12 terminal acrylic double bonds, is shown in Fig. 4. The ellipsoidal architecture of hyperbranched polymers has been considered to cause errors in the measurement of molecular weight by GPC methods, which calibrates using linear polystyrene as a standard. Therefore, in GPC measurements, molar mass for hyperbranched polymers is expected to be lower because of their smaller radius of chain gyration than the linear counterparts [26]. In this work, the weight average molecular weight of HPIP-A was experimentally measured to be 1.960 g mol^{-1} by GPC, compared with its theoretically calculation value of 2.450 g mol^{-1}. The wide molecular weight distribution of 2.05 was not only due to the high steric hindrance resulting from the dense aromatic rings, but also due to the statistics of the reactions in the system.

Naturally, the most important feature of a hyperbranched prepolymer is its DB, which has been defined by Fréchet and co-workers [27],

$$\mathrm{DB} = \frac{\text{dendritic units} + \text{terminal units}}{\text{dendritic units} + \text{terminal units} + \text{linear units}}$$

The established methods for measuring DB traditionally involve both NMR and functionalization-degradation methods [28,29]. In the NMR method, several model compounds with low molar mass, resembling the repeating units of a hyperbranched prepolymer, are usually synthesized. Based on the different NMR peaks of model compounds, the spectrum of a hyperbranched polymer can be assigned and the DB can be calculated from the integrals of those peaks.

From the ^{1}H NMR spectra of the model compounds as shown in Fig. 5, the resonances at 8.76, 8.42 and 8.32 ppm are assigned to the β protons, which have different structural

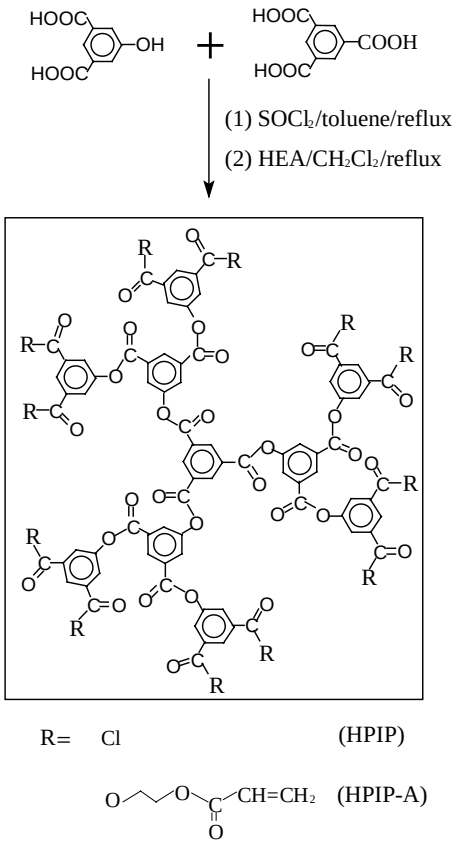

Fig. 4. Reaction scheme for the synthesis of HPIP-A ideally containing 12 terminal acrylic double bonds.

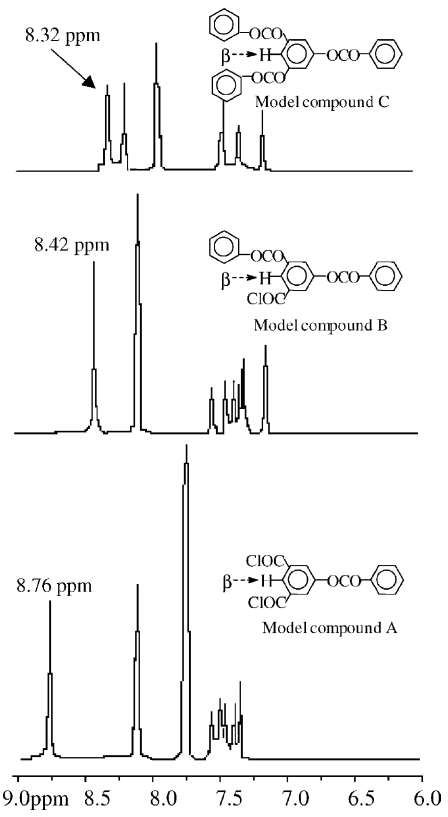

Fig. 5. ^{1}H NMR spectra of three model compounds.

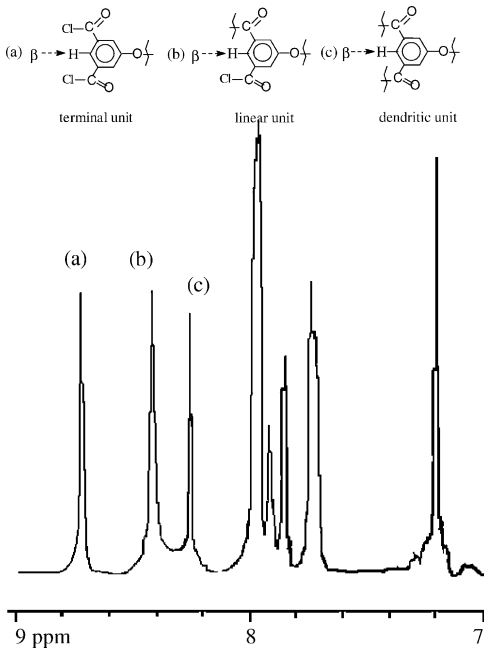

Fig. 6. ^{1}H NMR spectrum of HPIP endcapped with acyl chloride groups.

environments, in model compound A, B and C, respectively. HPIP molecule contains the similar structures of "terminal unit" with two free acyl chloride groups, "linear unit" with one free acyl chloride group and one benzoyl ester group, and "dendritic unit" with two benzoyl ester groups, as separately shown in Fig. 6. It is, therefore, possible to determine the relative amounts of model compound A, B and C in the ^{1}H NMR spectrum of HPIP based on the different resonances of β protons. The ^{1}H NMR spectrum of HPIP has shown a set of the resonances for different units appeared in the regions at 8.78–8.74, 8.45–8.39 and 8.34–8.30 ppm, respectively. Consequently, these resonances are assigned to the corresponding protons of the terminal units, linear units and dendritic units, respectively. Their relative amounts can be determined by integrating each region in the ^{1}H NMR spectrum. The DB of 0.45 for HPIP was, therefore, determined according to its definition, which is a general scale for hyperbranched polymers prepared by "one-pot" procedure [22].

3.1.2. Unsaturation concentration

As shown in Fig. 7, the integral of all areas assigned to Ar–H at the range of 9.15–7.84 ppm in the ^{1}H NMR spectrum of HPIP-A was used as an internal standard. The integral of all areas assigned to acrylic unsaturation at the range of 6.45–5.73 ppm, was used to determine the unsaturation concentration. Consequently, the unsaturation concentration of 5.29 $mmol_{C=C}\ g^{-1}$ for HPIP-A was obtained, compared with that of 5.60 $mmol_{C=C}\ g^{-1}$ by theoretically calculation.

3.1.3. Compatibility with monomer

The softening point (T_s) is defined as the extrapolated onset of the drop of log(E'). The glass transition temperature

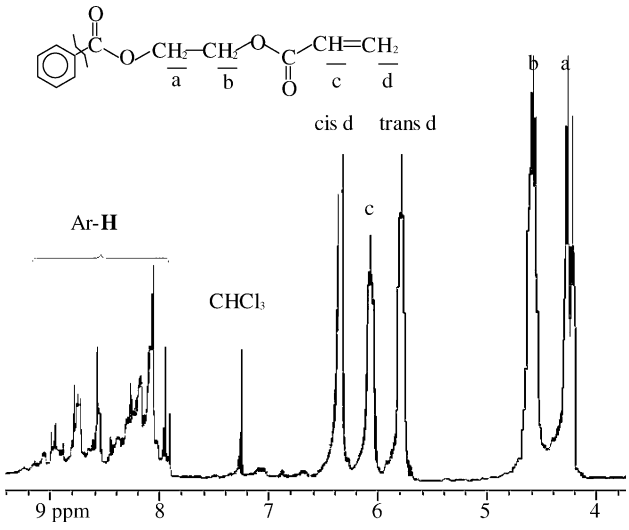

Fig. 7. ^{1}H NMR spectrum of the HPIP-A.

(T_g) is defined as the peak of Tan(δ) curve. The T_s/T_g ratio expresses the width of Tan(δ) peak, which is a rule that a higher T_s/T_g ratio leads to a narrow Tan(δ) peak and the film is more homogeneous. The dynamic mechanical thermal properties of these UV-cured films are shown in Figs. 8 and 9. It can be seen that the T_s/T_g values of these cured HPIP-A films without and with 20 and 40 wt.% monomer (MA) addition demonstrate that the three systems have the similar homogeneity. The data is listed in Table 1. This further proves HPIP-A has good compatibility with monomers.

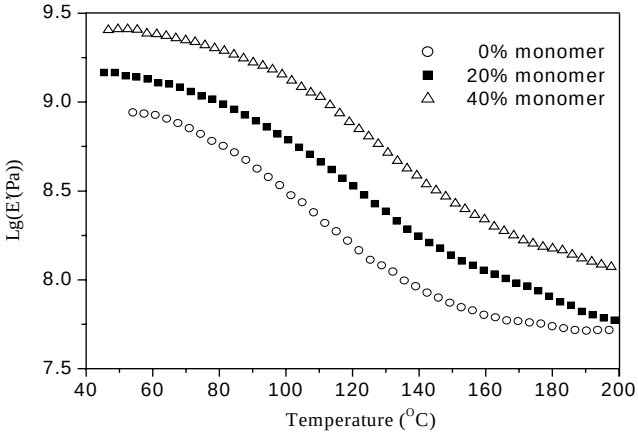

Fig. 8. Log E' curves of the UV-cured HPIP-A films as a function of MA content.

Table 1
Data of dynamic mechanical thermal analysis of the UV-cured HPIP-A films with and without monomer addition

Sample	T_s (°C)	T_g (°C)	T_s/T_g
HPIP-A	69	108	0.898
HPIP-A + 20 wt.% monomer	81	130	0.878
HPIP-A + 40 wt.% monomer	95	145	0.880

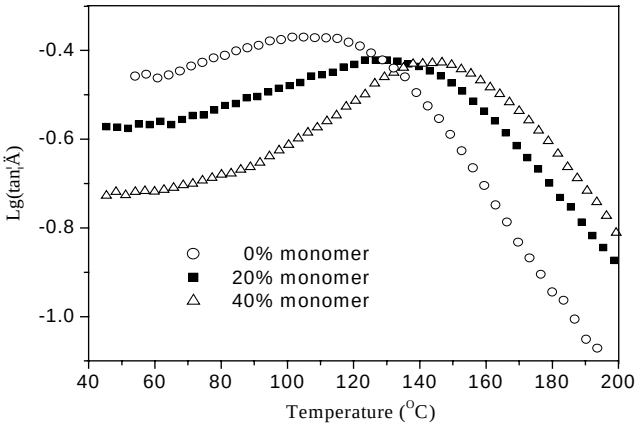

Fig. 9. Tan(δ) curves of the UV-cured HPIP-A films as a function of MA content.

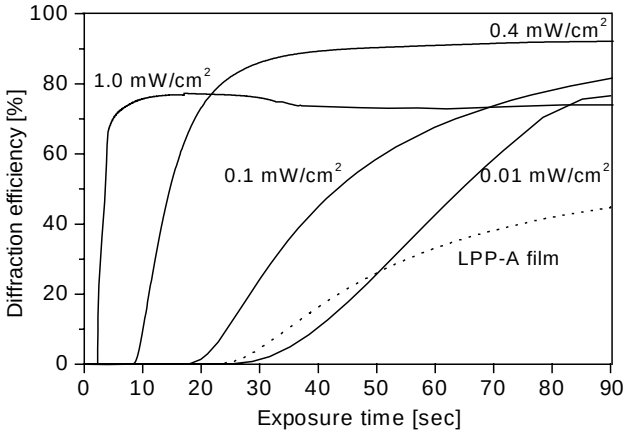

Fig. 11. Diffraction efficiency for 25 μm thickness HPIP-A films with 30 wt.% MA at different writing beam intensities.

3.1.4. Refractive index

As shown in Fig. 10, the RI of 1.562 for HPIP-A at the wavelength of 650 nm was determined by an autoretarder ellipsometer, compared with 1.564 for HPIP, endcapped with phenyl groups, developed by author [25]. The favorable RI value is achieved due to the presence of numerous benzene ring groups in the molecular structure. The higher the RI of a polymeric binder is, the more multifold monomers possessing low RI can be easily selected.

3.2. Influence factors on diffraction efficiency

3.2.1. Writing beam intensity

Fig. 11 shows the DE at different writing beam intensities measured using 25 μm thickness HPIP-A film with 30 wt.% MA. The curves present typical features of a free-radical photopolymerization process. The duration of initiation phase shortens with increasing the writing beam intensity, even disappears at the writing beam intensity of 1.0 mW cm^{-2}, as expected in free-radical polymerization systems [30]. At the writing beam intensities lower than 0.4 mW cm^{-2}, the diffusion rate of monomer MA exceeds its photopolymerization rate. As the photopolymerization proceeds, more monomers diffuse from the darker regions to the brighter ones. As a result, the modulation index Δn, together with the DE, increases with increasing the writing beam intensity. However, at higher writing beam intensity, such as 1.0 mW cm^{-2}, the photopolymerization rate of monomer exceeds its diffusion rate, which produces a decrease in DE compared with that at 0.4 mW cm^{-2}. This is because the high-crosslinked polymeric network formed at the initial phase impedes the further diffusion of the unreacted monomers. Moreover, the saturation exposure dose, defined as the exposure intensity multiply exposure time (s) at which the steady-state DE reached, of 36 mJ cm^{-2} was observed for this film. This value is far lower than that of 80 mJ cm^{-2} for DuPont photopolymer used by Curtis [14].

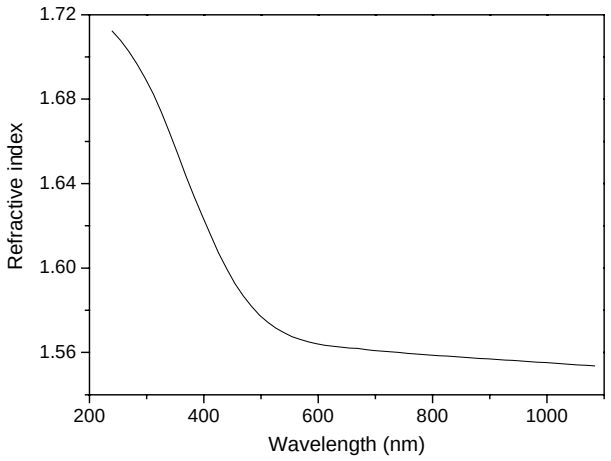

Fig. 10. Refractive index of HPIP-A vs. wavelength.

In order to investigate the effect of polymeric binder structures on diffraction gratings, the DE of 25 μm thickness LPP-A film with 30 wt.% MA was measured at the writing beam intensity of 0.4 mW cm^{-2}. The weight average molecular weight of 2.044 g mol^{-1} and polydispersity of 1.45 for LPP-A was experimentally obtained by GPC measurement. The higher RI of 1.587 for LPP-A was obtained, compared with that of 1.562 for HPIP-A. However, the lower DE of 45.6% for LPP-A film was obtained, compared with that of 92.3% for HPIP-A film. Moreover, the steady-state DE of the former reached after longer exposure time. This may be explained by the fact that the higher viscosity of LPP-A, resulting from its inter/intra-molecular chain entanglements, impedes the diffusion of unreacted monomers during the recording process. This implies that hyperbranched prepolymers are more competitive than linear prepolymers used in photopolymerizable recording dry films as polymeric binders.

3.2.2. Film thickness

The DE for the various thickness HPIP-A films with 30 wt.% MA at the writing beam intensity of 0.4 mW cm^{-2}

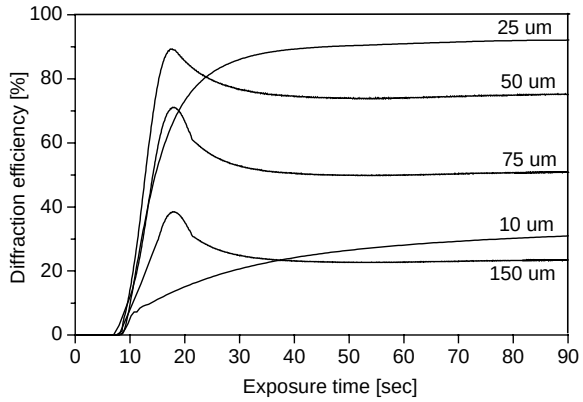

Fig. 12. Diffraction efficiency for the various thickness HPIP-A films with 30 wt.% MA at the writing beam intensity of 0.4 mW cm^{-2}.

is shown in Fig. 12. The distinct increase of DE is observed when the film thickness increases from 10 to 25 μm. This can be explained with the theoretical description of DE (η) for volume holograms, which is given as:

$$\eta = \sin^2\left[\frac{\pi d\,\Delta n}{\lambda\cos(\theta)}\right]$$

where d is the film thickness and λ is the wavelength of probe beam. An estimate based on this model gives the Δn value of 10^{-2}. However, this behavior is reversed when the film thickness further increases, as summarized in Table 2. For the 50 μm thickness film, the maximum DE (η_{max}) is observed for the exposure time of about 20 s, followed by a decrease to the steady-state DE (η_{st}) after longer exposure. For the 75 and 150 μm thickness films, the same behavior performs more remarkably. The value of η_{st}/η_{max} decreases with increasing the film thickness. This can be assumed that the light scattering takes place whilst the copolymerization of HPIP-A and monomers occurs, which results in the destruction of periodic intensity distribution of the writing beams as well as their mutual coherence. As a result, the diffraction beam may broaden, which becomes more obvious at the film thicknesses of over 50 μm. This broadening results in a decrease of the recorded diffraction intensity, because a part of it falls out of the view field of the detector. Moreover, the light scattering-induced grating destruction can be also understood by the diffusion of unreacted monomers. When the writing beam passes through a thicker film, its intensity decreases with increasing the incident depth due to the light scattering and/or absorption. This leads to the inhomogeneous polymerization and a viscosity gradient in the film depth. Therefore, the decrease of Δn is induced by means of the diffusion of unreacted monomers from the bottom layer to the top layer of a thicker film. Therefore, it can be concluded that the thickness of a recording dry film should not exceed 25 μm to avoid light scattering-induced grating destruction.

Table 2
η_{max} and η_{st} values for the various thickness HPIP-A films with 30 wt.% MA at the writing beam intensity of 0.4 mW cm^{-2}

	Film thickness (μm)				
	10	25	50	75	150
η_{max} (%)	31.5	92.3	89.6	71.6	38.9
η_{st} (%)	31.5	92.3	75.4	51.1	22.7
η_{st}/η_{max} (%)	–	–	83.1	71.4	58.4

3.2.3. Monomer structure and content

In order to substantiate the photopolymerization–diffusion model during the formation of holographic diffraction gratings in these photopolymerizable recording dry films, five monomers (MA, MMA, HEA, HDDA and TMPTA) with different diffusion performance were selected as the components of these curable films. Fig. 13 shows the DE for 25 μm thickness HPIP-A films with 30 wt.% different monomers at the writing beam intensity of 0.4 mW cm^{-2}. It can be found that the DE decreases with increasing the functionality of monomers. This is because the high crosslinked polymeric network formed rapidly by the copolymerization of HPIP-A and multifunctional monomers, HDDA and TMPTA, impedes the further diffusion of unreacted monomers from darker regions to brighter ones in a larger extent. Furthermore, the bulky molecular structure of TMPTA leads to its poor diffusion performance. Moreover, the DE curves for HPIP-A films with MA and MMA level up in shorter periods. For the different monofunctional monomers MA, MMA and HEA, the DE of 32.7% for the film with HEA is much lower than those of 92.3, 77.4% for the films with MA and MMA, respectively. This may be interpreted that the polarity of HEA leads to poor compatibility with HPIP-A, as well diffusion property. This substantiates the photopolymerization–diffusion model of these systems.

The DE for the 25 μm thickness HPIP-A films with different MA contents at the writing beam intensity of 0.4 mW cm^{-2} is shown in Fig. 14. The distinct increase in DE is observed when the MA content increases from 20 to 30 wt.%. This can be explained that 20 wt.% monomer in the resin is not enough to obtain a considerable Δn, as

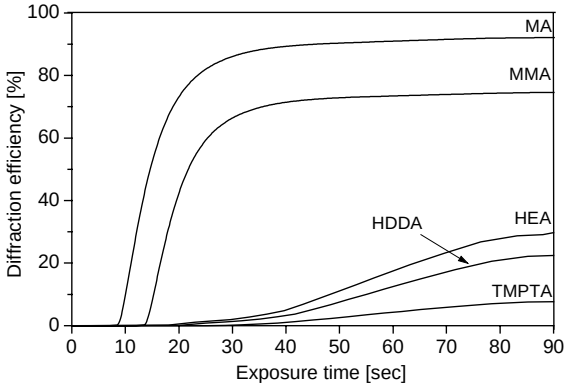

Fig. 13. Diffraction efficiency for 25 μm thickness HPIP-A films with 30 wt.% different monomers at the writing beam intensity of 0.4 mW cm^{-2}.

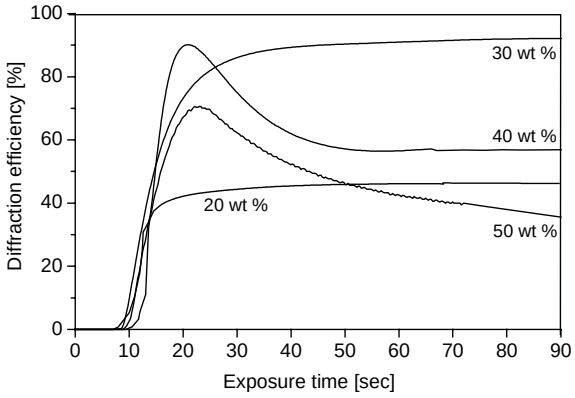

Fig. 14. Diffraction efficiency for 25 μm thickness HPIP-A films with different MA contents at the writing beam intensity of 0.4 mW cm^{-2}.

Table 3
η_{max} and η_{st} values for 25 μm thickness HPIP-A film with different MA contents at the writing beam intensity of 0.4 mW cm^{-2}

MA content (wt.%)	20	30	40	50
η_{max} (%)	46.1	92.3	90.2	70.2
η_{st} (%)	46.1	92.3	56.7	35.9
η_{st}/η_{max} (%)	–	–	62.9	51.1

well DE. However, the η_{max} is observed for the 40 wt.% MA film after 20 s exposure, followed by a decrease to the lower η_{st} when exposed for over 45 s. This behavior becomes more obvious when the monomer content further increases. For the 50 wt.% MA film, the lower values of η_{max} and η_{st} compared with the film containing 40 wt.% MA are obtained. The value of η_{st}/η_{max} decreases with increasing the MA content, as listed in Table 3. This may be explained by the fact that high monomer contents lead to the scattering-induced destruction more obviously.

4. Conclusions

HPIP-A theoretically endcapped with 12 terminal acrylic double bonds per molecule was synthesized from BTCA, HIPA and HEA, proceeding in a “one-pot” procedure. A high RI of 1.562 at the wavelength of 650 nm for the obtained prepolymer was determined by an ellipsepsometer. The study on the holographic diffraction gratings has shown that the DE is strongly dependent on the writing beam intensity, film thickness, monomer structure and content. For the 25 μm thickness film, the higher DE of 92.3% and the Δn of 10^{-2} were obtained at the writing beam intensity of 0.4 mW cm^{-2}. For the thicker films of over 25 μm, the η_{max} was observed when exposed for about 20 s, then followed by a decrease to the lower η_{st} after further exposure. This phenomenon becomes more obvious with increasing the film thickness and monomer content. The functionality and polarity of monomers have significant influence on DE. Therefore, it can be concluded that the 25 μm thickness HPIP-A film with 30 wt.% MA is recommended to prepare the holographic diffraction grating with a higher DE at the writing beam intensity of 0.4 mW cm^{-2}.

References

[1] C. Carre, D.J. Lougnot, Y. Renotte, P. Leclere, Y. Lion, J. Opt. 23 (1992) 73–79.
[2] L. Dhar, K. Curtis, M. Tackitt, M. Schilling, S. Campbell, W. Wilson, A. Hill, C. Boyd, N. Levinos, A. Harris, Opt. Lett. 23 (1998) 1710–1712.
[3] G.J. Steckman, I. Solomatine, G. Zhou, D. Psaltis, Opt. Lett. 23 (1998) 1310–1312.
[4] R.M. Shelby, D.A. Waldman, R.T. Ingwall, Opt. Lett. 25 (2000) 713–715.
[5] S. Martin, P. Leclere, Y.L.M. Renotte, V. Toal, Y.F. Lion, Opt. Eng. 33 (1994) 3942–3946.
[6] I. Benjamin, H. Hong, Y. Avny, D. Davidov, R. Neumann, J. Mater. Chem. 8 (1998) 919–924.
[7] L. Dhar, M.G. Schnoes, T.L. Wysocki, H. Bair, M. Schilling, C. Boyd, Appl. Phys. Lett. 73 (1998) 1337–1339.
[8] T.J. Trentler, J.E. Boyd, V.L. Colvin, Chem. Mater. 12 (2000) 1431–1438.
[9] M.M. Wang, S.C. Esener, Appl. Opt. 39 (2000) 1826–1834.
[10] G.J. Steckman, Opt. Lett. 25 (2000) 607–609.
[11] J.R. Lawrence, F.T. O’Neill, J.T. Sheridan, Optik 112 (2001) 449–463.
[12] S. Blaya, L. Carretero, R.F. Madrigal, M. Ulibarrena, A. Fimia, Appl. Phys. B 74 (2002) 603–605.
[13] V. Moreau, Y. Renotte, Y. Lion, Appl. Opt. 41 (2002) 3427–3435.
[14] K. Curtis, D. Psaltis, Appl. Opt. 33 (1994) 5396–5399.
[15] P. Jordan, F. Marquis-Weible, Appl. Opt. 35 (1996) 6146–6150.
[16] I. Aubrecht, M. Miler, I. Koudela, J. Mod. Opt. 45 (1998) 1465–1477.
[17] S. Blaya, L. Carretero, R.F. Madrigal, A. Fimia, Opt. Commun. 173 (2000) 423–433.
[18] R.R. Adhami, D.L. Lanteigne, D. Gregory, Microwave Opt. Tech. Lett. 4 (1991) 106–109.
[19] P. Ayräs, J.T. Rantala, S. Honkanen, S.B. Mendes, N. Peyghambarian, Opt. Commun. 162 (1999) 215–218.
[20] W.J. Tomlinson, E.A. Chandross, Adv. Photochem. 12 (1980) 201–208.
[21] D.J. Lougnot, C. Turch, C. Leroy-Garel, Proc. SPIE 3417 (1998) 165–171.
[22] A. Hult, M. Johansson, E. Malmström, Adv. Polym. Sci. 143 (1999) 1–34.
[23] A.W. Freeman, J.M.J. Fréchet, Org. Lett. 1 (1999) 685–687.
[24] S.R. Turner, F. Walter, B.I. Voit, T.H. Mourey, Macromolecules 27 (1994) 1611–1616.
[25] H.G. Kou, A. Asif, W.F. Shi, Synthesis and characterization of hyperbranched aromatic polyesters used for polymeric graded-index materials, Polym. Int. 52 (2003) 1088–1094.
[26] T.H. Mourey, S.R. Turner, M. Rubinstein, J.M.J. Fréchet, C.J. Hawker, K.L. Wooley, Macromolecules 25 (1992) 2401–2406.
[27] C.J. Hawker, R. Lee, J.M.J. Fréchet, J. Am. Chem. Soc. 113 (1991) 4583–4588.
[28] D.H. Bolton, K.L. Wooley, Macromolecules 30 (1997) 1890–1896.
[29] E. Malmström, M. Johansson, A. Hult, Macromolecules 28 (1995) 1698–1703.
[30] E. Andrzejewska, M.A. Andrzejewski, J. Polym. Sci. Part A: Polym. Chem. 36 (1998) 665–673.